ESP-JETA
ESP Journal of Engineering & Technology Advancements
ISSN: 2583-2646 / Volume 3 Issue 4 December 2023 / Page No: 36-44
Paper Id: JETA-V3I8P104 / Doi: 10.56472/25832646/JETA-V3I8P104

Original Article

Prediction and Optimization of Chip Removal Rate Required to enhance the Weld's Tool Life using Response Surface Methodology (RSM) and Artificial Neural Network (ANN)

Eyituoyo Amorighoye Lucky[1], Achebo Joseph[2], Obahiagbon Kessington[3], Uwoghiren Frank Omos[4]

[1,2,4]*Department of Production Engineering, University of Benin, Benin City, Nigeria.*
[3]*Department of Chemical Engineering, University of Benin, Benin City, Nigeria.*

Received Date: 03 November 2023 Revised Date: 18 November 2023 Accepted Date: 01 December 2023

Abstract: *The rise in the failure of mechanical components, some of which are attributable to poor weld joints has given rise to research study on the optimization of weld joint strengths. Irrespective of the welding process, the need for the right combination of input process parameters cannot be over emphasized. To achieve a desired weld quality, a weld mechanical property such as the Chip Removal Rate was examined and related to weld input parameters such as depth of cut, cutting speed and feed rate. The Response Surface Methodology (RSM) and Artificial Neural Network (ANN) were used to predict and optimize the Chip Removal Rate of a required to enhance the tool life of some Selected Material. Model adequacy checks, was done using analysis of variance (ANOVA) and found to be adequate. The experimental setup adheres to the central composite design, meticulously constructed using Design expert software (version 13.0). The Response Surface Methodology analysis yields optimal outcomes, depth of cut of 0.400mm, cutting speed of 250m/min and feed rate of 0.5Mm/rev. These parameters collectively yielded a welded joint with chip removal rate of 8.638 Mm/min achieving a desirability value of 0.973. In the Artificial neural network (ANN), 70% of the data was used for training, 15 % was used for validating and the remaining 15% for the actual test. From the results obtained, the RSM in this case had better predicted values. The findings underscore the pivotal role of optimizing non-elastic performance factors in weldment joints. The study showcases performance factors critical for augmenting the strength and structural integrity of machined components.*

Keywords: *Weld Joint, Chip Removal Rate, Response Surface Methodology, Artificial Neural Network.*

I. INTRODUCTION

Machining involves using cutting tools to shape raw materials, producing a workpiece with specified dimensions and desired properties. Machining is extensively used because of its capability to shape intricate geometries, achieve precise dimensions and surface deviations, and utilize unique cutting tools that enable diverse operational possibilities [1]. The production of equipment elements from reinforced steels or white cast irons involves use of conventional machining techniques such as turning, heat treatment, and grinding. Depending on the final shape that the grinding process yields, there are a number of benefits to manufacturing parts by hard machining. In particular, there are several benefits to hard turning, including quick production times and high chip removal rates [2]. In machining operations, chip removal rate is a critical parameter that influences tool life, machining efficiency, and productivity. Achieving an optimal chip removal rate is essential for reducing tool wear, increasing tool life, and ensuring cost-effective manufacturing [3]. Optimizing the chip removal rate is vital in machining processes as it affects many facets of machining, particularly like heat production, surface finish, slicing pressures, and tool damage. An optimal chip removal rate can result in lower production costs, longer tool life, and enhanced overall machining efficiency. Different materials exhibit distinct behaviors during machining, necessitating tailored approaches for chip removal rate optimization [4]. Experimental validation is a key aspect of chip removal rate optimization research. Researchers conduct experiments to measure the chip removal rate, finishes on the surface, heating, slicing forces, and tool wear during various machine conditions. Empirical data are essential for validating and refining chip removal rate optimization models. Predictive models play a pivotal role in optimizing the chip removal rate. These models use mathematical equations, empirical data, or computational simulations to predict the chip removal rate based on cutting parameters, material properties, tool geometry, and machining conditions [5]. In manufacturing, there is a growing demand for increased productivity, especially in machining processes. Concurrently, there's a push for workshops to minimize energy wastage throughout the blade-cutting process [7]. [8]

investigated utilizing three multi-objective optimization methods (TOPSIS - Technique for Order Performance by Similarity to Ideal Solution, DEAR - Data Envelopment Analysis Ranking, and GRA - Grey Relational Analysis) that rely on the signal-to-noise (S/N) ratio, with the aim to determine the most advantageous technical specifications. These parameters are linked to the arithmetic mean roughness (Ra), insert wear (Vb), and chip removal rate while turning a refractory alloy using a composite ceramic cutting tool (CC670). Also, [9] investigated the influence of low-frequency and high-amplitude vibrations on chip formation in age-hardened copper-zirconium for small diameters as diminutive as 0.94 mm and L/D ratios reaching up to 40. Implementing affordable and energy-saving methods for removing chips is crucial for sustainability [10]. According to [11], minimizing chip depth, surface imperfections and cutting temperature is necessary to achieve better machining, while concurrently increasing the material removal rate. [12] found that the relationship between spindle velocity and depth-of-cut has substantial impact on the rapid removal of chips from the workpiece in lubricated environments. As drilling depth grows in deeper bore drilling procedures, the limited area for chip evacuation causes chip deposition inside the drill flutes as drilling bore becomes deeper. Consequently, drill breakage could result from this accumulation of high drilling pressure. [13] studied the impact of the chip removal process during peck drilling on the drilling depth. The extended depth coefficient by chip removal was introduced by [13] to establish the relationship between the total drilling depth and the extended depth of each drilling stage. It has been demonstrated that when using carbide tools to machine titanium alloy Ti6Al4V, the position angle is advantageous economically because it reduces the machining time while keeping the same rate of chip removal; it has no impact on the force model [14]. In rough milling operations, serrated cutting tools were developed to remove chips more effectively [15]. [15] conducted a closely monitored investigation into the theoretical and experimental aspects of chip morphology and removal during the titanium alloy drilling technique aided by low-frequency vibration.. In a study by [16], Ti6Al4V's ability to be machined was assessed in both MQCL and MQL scenarios. Their findings indicated that MQCL exhibited superior processing performance compared to MQL. In addition to reducing the cutting temperature, using cold air improved the lubricating qualities of the cutting fluid and accelerated the chip removal process. Optimizing chip removal rate is a fundamental aspect of machining operations with significant implications for tool life, efficiency, and product quality.

II. METHODOLOGY

A. Research Design:

In this particular research investigation, based on the number of input parameters, an experimental design was developed. The matrix was created using software designed for experts in design. The central composite design (CCD) and the 2k factorial design were employed. The 2^k factorial design is for any number of input parameters considered at 2 levels while the CCD is for any input parameters considered within the range of 3- 5 levels.

B. Method of Data Collection:

Using the design 7.1 program, the central composite design for this investigation was created, producing 20 runs for the experiment. The findings of the chosen material as well as input and output parameters were included in these test runs. This matrix was then analyzed.

C. Response Surface Methodology (RSM):

RSM are extensively used in situations where there are many input factors that may influence one or more response variables. Response Surface Methodology (RSM) examines processes where a desired outcome is influenced by several variables, with the primary goal of optimizing this outcome. It does this by combining mathematical and statistical models. Additionally, it holds significant relevance in crafting, evolving, and composing new product designs, and enhancing the current product formulations. The fundamental elements of response surface methodology encompass experimental design, regression analysis, and optimization algorithms, utilized to explore empirical relationships.

D. Artificial Neural Network:

Response Surface Methodology (RSM) techniques were employed to investigate this matrix. A neural network represents a highly parallel and distributed computing system, it has the capacity to retain experimental data for various applications. It functions as a data mining tool and is primarily designed to uncover hidden patterns within datasets. Interestingly, there are two key similarities between neural networks and the human brain. First, during the learning process within the network, synaptic weights are employed to store knowledge. These weights indicate the strength of connections between internal neurons. Second, each basic neuron with R inputs receives appropriate weights (w), and the transfer function (f) calculates the total of these weighted inputs along with a bias term. The transfer function (f) can be any differentiable function used to determine neuron results. In multilayer networks, the log-sigmoid transfer function, often referred to as logsig, is commonly used. The sigmoid

transfer function, specifically the log-sigmoid, generates output. As the net input of the neuron transitions from a negative value to positive infinity, the values vary within the range of 0 to 1.

III. RESULTS AND DISCUSSION

In this research, a total of 20 experimental trials were conducted, with each trial involving adjustments to the depth of cut, spindle speed, and feed rate. During each experiment, the corresponding responses were carefully measured.

A. Modelling and Optimization using RSM:

To check for model suitability, the sequential sum of squares for chip removal rate response is shown in Table 1.

Table 1: Sum of Squares in a Sequential Model Chip Removal Rate

Source	Sum of Squares	df	Mean Square	F-value	p-value	
Mean vs Total	862.25	1	862.25			
Linear vs Mean	50.29	3	16.76	2.93	0.0657	
2FI vs Linear	33.26	3	11.09	2.47	0.1082	
Quadratic vs 2FI	**54.95**	**3**	**18.32**	**53.20**	**< 0.0001**	**Suggested**
Cubic vs Quadratic	1.13	4	0.2821	0.7312	0.6026	Aliased
Residual	2.31	6	0.3858			
Total	1004.19	20	50.21			

Choose the highest order polynomial in which the model is not aliased and the extra terms have substantial meaning.

In order to determine the most appropriate model for the Chip Removal Rate, a lack of fit test was conducted, and the model exhibiting the least significant lack of fit was chosen. Table 2 displays the lack of fit analysis for the Cutting Force.

Table 2: Lack of Fit Tests Chip Removal Rate

Source	Sum of Squares	df	Mean Square	F-value	p-value	
Linear	89.44	11	8.13	18.38	0.0024	
2FI	56.18	8	7.02	15.88	0.0037	
Quadratic	**1.23**	**5**	**0.2463**	**0.5569**	**0.7319**	**Suggested**
Cubic	0.1032	1	0.1032	0.2333	0.6495	Aliased
Pure Error	2.21	5	0.4423			

The chosen model should exhibit a lack of fit that is deemed insignificant.

To further assess the appropriateness of the model, the summary statistics for the Chip Removal Rate were examined, favoring the model with the highest coefficient of determination. The model summary statistics for the Chip Removal Rate are presented in Table 3.

Table 3: Model Summary Statistics Chip Removal Rate

Source	Std. Dev.	R^2	Adjusted R^2	Predicted R^2	PRESS	
Linear	2.39	0.3543	0.2332	-0.1374	161.45	
2FI	2.12	0.5886	0.3988	0.1452	121.34	
Quadratic	**0.5868**	**0.9757**	**0.9539**	**0.9052**	**13.45**	**Suggested**
Cubic	0.6211	0.9837	0.9484	0.8173	25.93	Aliased

Concentrate on the model that optimizes both the predicted and adjusted R2.

To check for the strength of the model developed the goodness of fit statistics test is done for chip removal rate as shown in Table 5.

Table 5: Goodness of Fit Statistics for Chip Removal Rate

Std. Dev.	0.5868		**R^2**	0.9757
Mean	6.57		**Adjusted R^2**	0.9539
C.V. %	8.94		**Predicted R^2**	0.9052
			Adeq Precision	23.4851

The variation between the projected R2 of 0.9052 and the revised R2 of 0.9539 is less than 0.2, indicating a comparatively good agreement between the two. Adequate Precision evaluates the signal-to-noise ratio. A ratio above 4 is desirable, and your ratio of 23.485 signifies an adequate signal. This model is suitable for exploring the design space.

To show the model is suitability for the data with respect to Chip Removal Rate, a normal plot of residuals for Chip Size is shown in Figure 1.

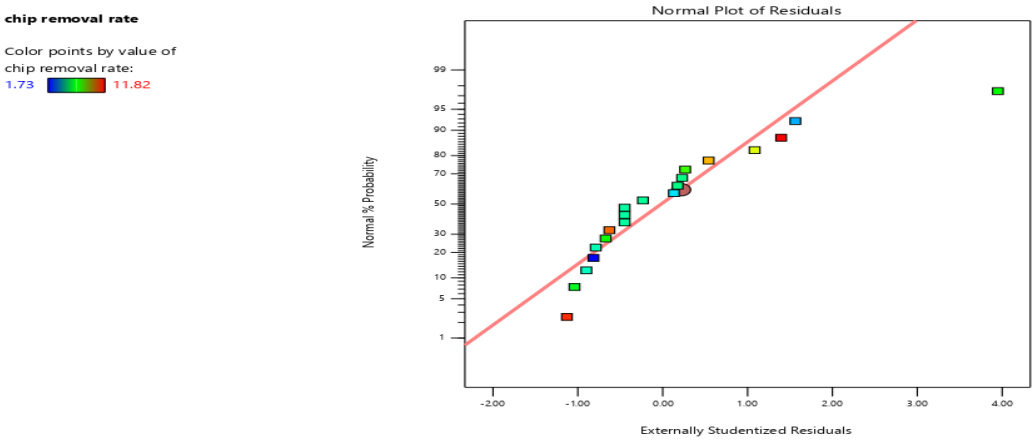

Figure 1: Residual Normal Plot for Chip Removal Rate

The normal probability plot serves to assess whether the residuals adhere to a normal distribution, where the points should align along a straight line. Even a moderate dispersion is linked to normally distributed data. The normal plot of residuals Chip Removal Rate revealed a moderate scatter indicating that the data is normal.

Figure 2 illustrates the plot of residuals and anticipated values for Chip Removal Rate that was created in order to look for the presence of massive patterns or expanding variance.

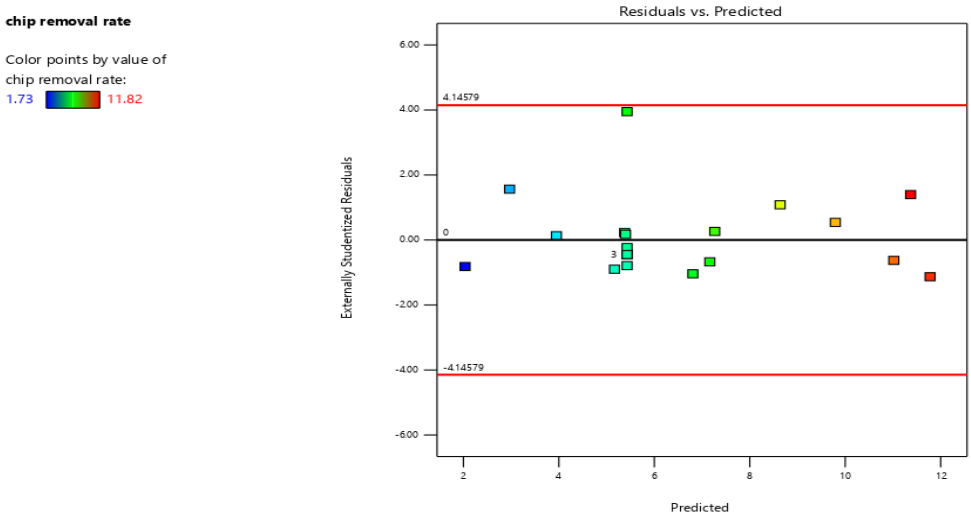

Figure 2: Residual vs. Predicted Plot for Chip Removal Rate

To pinpoint potential anomalies within the experimental data, a Cook's distance plot was generated for the Chip Removal Rate. Cook's distance gauges the degree to which the regression outcome would change if an outlier were omitted from the examination. If a point is noticeably farther away from other points than the others, it can be an anomaly that needs more research. Figures 3 show the Cook's distance generated for Chip Removal Rate.

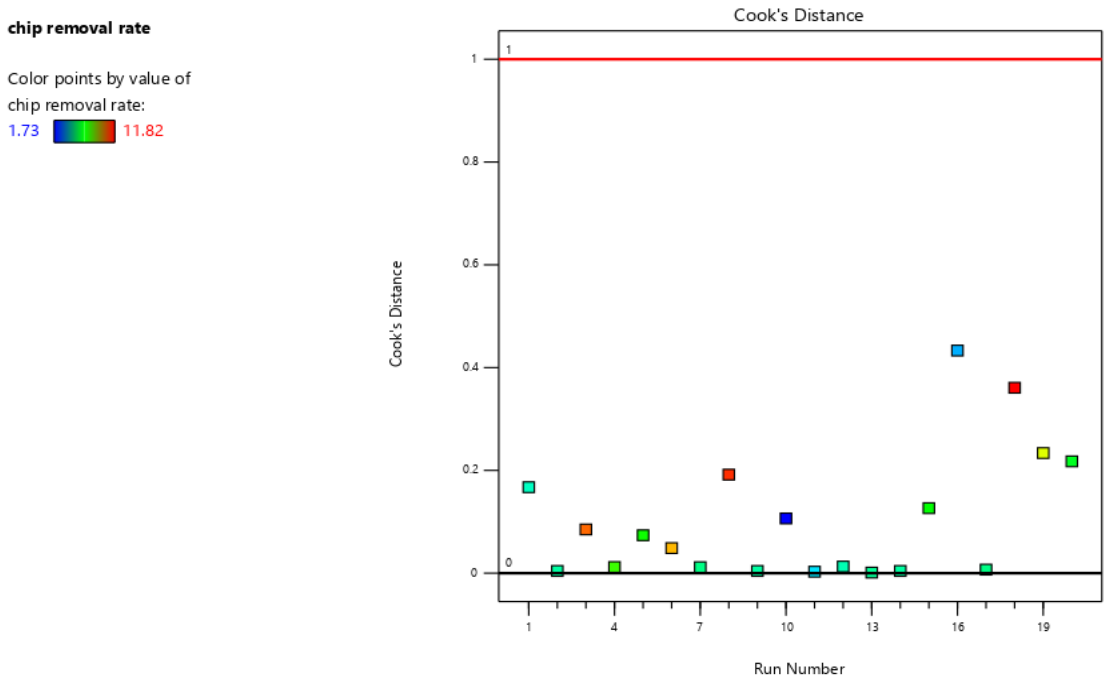

Figure 3: Cook Distance for Chip Removal Rate

The 3D Surface Plot in Figure 4A and 4B, illustrating the correlation between Cutting Speed and Depth of Cut against Chip Removal Rate, it is evident that augmenting Cutting Speed initially boosts the Chip Removal Rate. However, subsequent increments in Cutting Speed along with increasing Depth of Cut contribute to a reduction in the Chip Removal Rate.

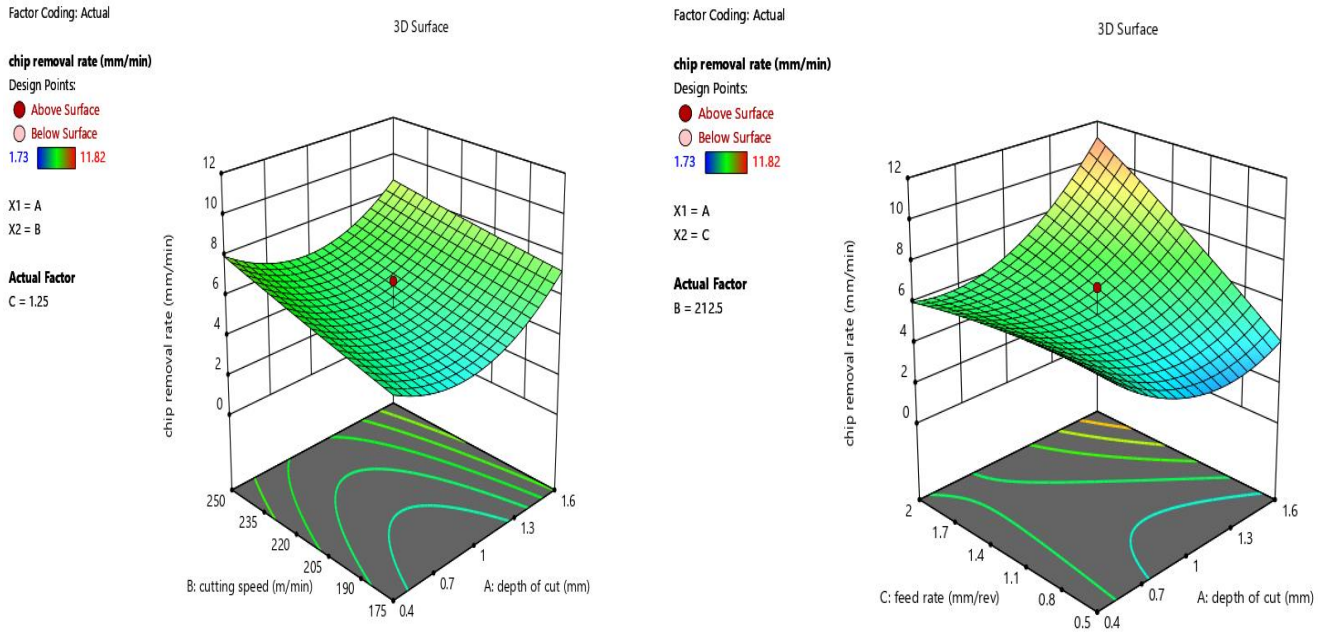

Figure 4: A. 3D surface plot of Cutting Depth and Speed B. 3D surface plot of feed rate and Depth of cut

The 3D surface plot presented in figure 5 showcases the influence of changes in feed rate and depth of cut on the chip removal rate. it highlights that elevating the feed rate corresponds directly to an increase in the chip removal rate. meanwhile, an initial increase in the depth of cut results in a reduction in the chip removal rate, followed by a slight subsequent increase.

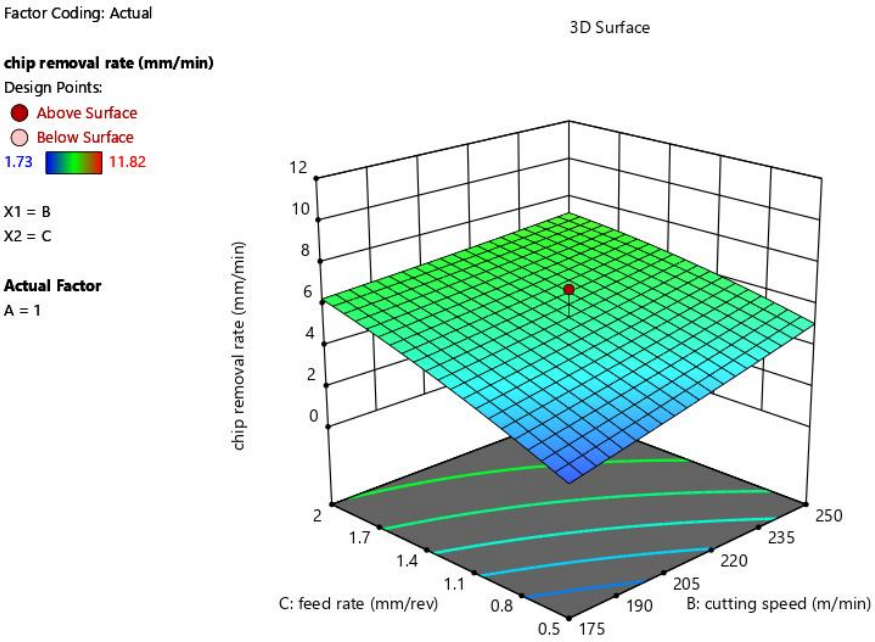

Figure 5: 3D surface plot Cutting Speed and Depth of Cut

The 3D surface plot which shows the effect of feed rate and cutting speed on the chip removal rate reveals that increase in feed rate and cutting speed result in the increase of the chip removal rate. However, the feed rate has a stronger effect on the chip removal rate.

B. Modelling and prediction using Artificial Neural Network (ANN)

MATLAB R2022a is used in the analysis for the Artificial neural network. The data is stored within the MATLAB folder and then converted into a numeric matrix format after normalization. This will immediately select the range of the dataset, and import selection is used to load the data into MATLAB. The superior second-order gradient method, recognized as the Levenberg-Marquardt Back Propagation training algorithm, was chosen as the optimal learning rule and subsequently implemented in the development of the network architecture. The network was configured with 15 neurons in each hidden layer, and its performance was tracked using the coefficient of determination (r2) and MSE. The input layer of the network applies the hyperbolic tangent (tan-sigmoid) transfer function to compute the layer output from the network input, while the output layer employs the linear (purelin) transfer function. The process of developing the network involves partitioning the input data into training, validation, and testing sets. In this research, with a maximum of 1000 training cycles, 70% of the data was used for network training, 15% for network validation, and the remaining 15% for network performance assessment. By employing Levenberg-Marquardt optimization, the Trainlm function adjusts weight and bias parameters during network training. This algorithm is renowned for its speed and is considered one of the swiftest backpropagation methods accessible. Trainlm is strongly suggested as the primary supervised algorithm, even though it demands more memory compared to other algorithms. This identical network architecture was devised to predict the chip removal rate as a sole response variable, utilizing three input variables as shown in Figure 6.

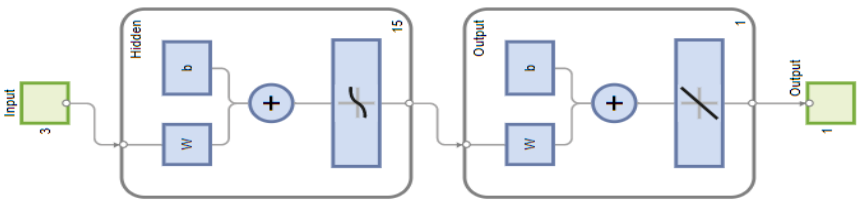

Figure 6: Artificial Neural Network Architecture

The Artificial Neural Network architecture follows a 3-15-1 configuration. The network diagram, created for the prediction of chip removal rate using the backpropagation neural network, is illustrated in Figure 7.

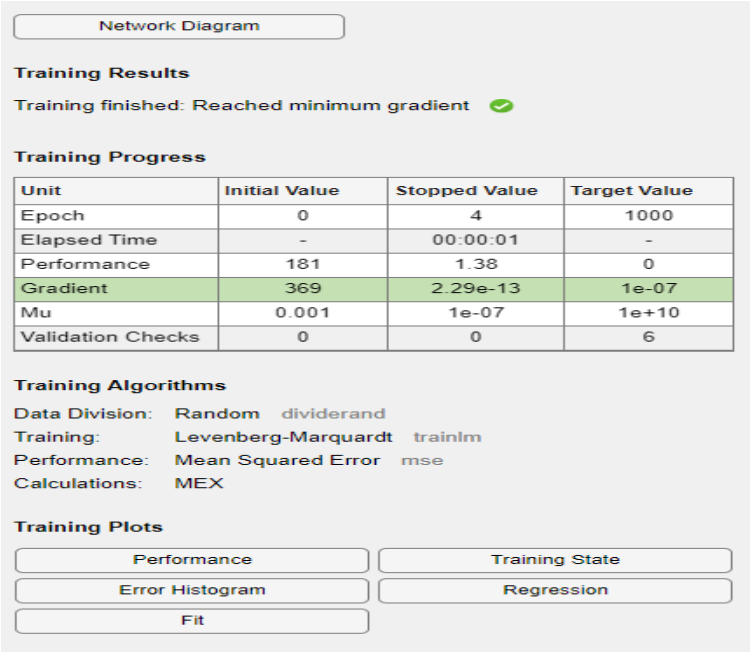

Figure 7: Model Summary for Predicting Chip Removal Rate

In the network training diagram depicted in Figure 7, it was noted that the network's performance stood at 181, with a validation check showing zero (0) out of six (6). This outcome was anticipated, considering that the normalization of the raw data had already addressed the issue of weight bias. The performance curve of trained network for predicting chip removal rate is shown in Figure 8. The training state, displaying the gradient function, training gain (Mu), and validation check, is depicted in Figure 9.

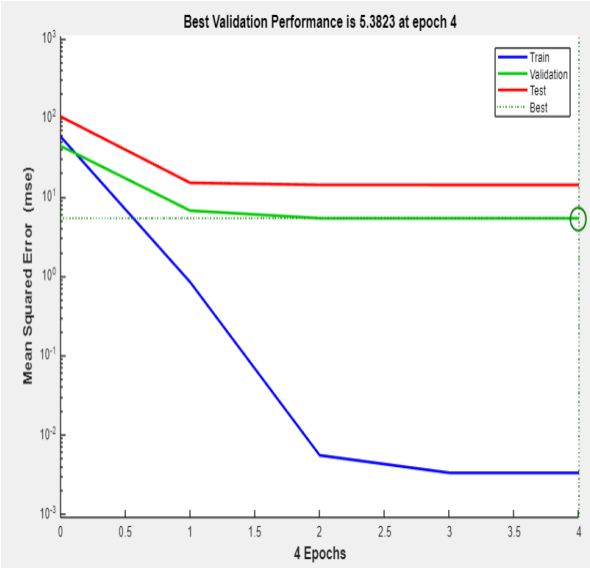

Figure 8: Performance Curve of Trained Network

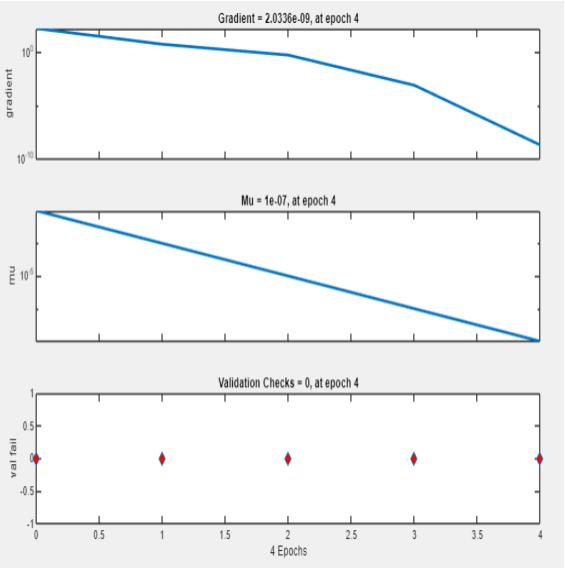

Figure 9: Neural Network Training State

From Figure 8, observing the performance curve, there was no indication of overfitting. Furthermore, a consistent pattern was noted in the behaviour of the training, validation, and testing curves, as anticipated due to the normalization of the raw data before use. A reduced square root error serves as a critical factor for assessing a network's training accuracy. While from Figure 9, an error value of 5.3823 at epoch 4 provides evidence of a network with robust predictive capabilities for chip removal rate. Backpropagation is an artificial neural network technique used to compute the erroneous contribution of each neuron after a batch of data training. Essentially, the neural network computes the loss function's gradient to clarify the mistake contributions made by each of the selected neurons. A lower error is preferred. The computed gradient value of 2.0336e-09, as depicted in Figure 15, indicates that the error contributions of each selected neuron are exceedingly minimal. The momentum gain (Mu) serves as the control parameter for the algorithm employed in training the neural network. It represents the training gains and must possess a value lower than unity. A momentum gain of 1e-07 demonstrates a network with a high capability to predict the chip removal rate. Figure 10 illustrates the regression plot correlating the input variables (DOC, cutting speed, and feed rate) with the target variable (chip removal rate), alongside the progress of training, validation, and testing.

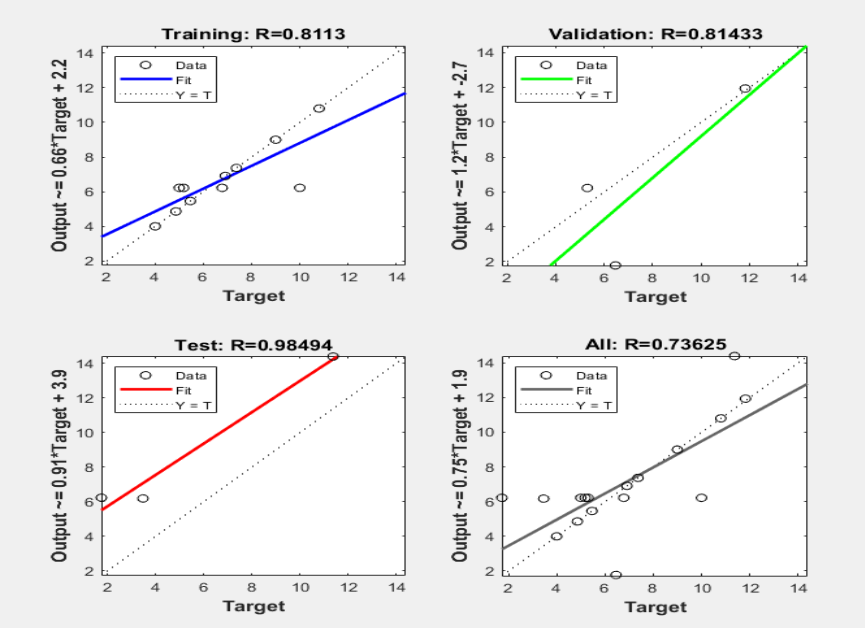

Figure 10: Plot displaying the Evolution of Training, Validation, and Testing

Upon examining the calculated values of the correlation coefficient (R) shown in Figure 16, the determination was made that the network has been effectively trained and is suitable for predicting the chip removal rate.

IV. CONCLUSION

A machined engineering structure's rate of chip removal affects how long it can operate. This investigation involves creating numerical models utilizing response surface techniques and artificial neural networks to forecast and improve the chip removal rate while taking the feeding rate, the degree of cut, and speed of cut into account. The experimental setup employed the central composite design, created using the Design 7.1 software. The response surface methodology (RSM) analysis resulted in optimal solutions, showing that a degree of cut of 0.400, cutting speed of 250.000, and feed rate of 0.500 produced a machined structure with a chip removal rate of 8.638, achieving a desirability value of 0.973. Furthermore, the design of artificially generated neural networks was utilized to forecast the output parameters and was compared with the RSM methodology. From the results obtained the response surface methodology is selected as the better predictive model over the Artificial Neural Network because it has a higher coefficient of determination.

V. REFERENCES

[1] Boumaza, H., Belhadi, S., Yallese, M. A., Safi, K., & Haddad, A. (2022). Optimization of surface roughness, tool wear and material removal rate in turning of Inconel 718 with ceramic composite tools using MCDM methods based on Taguchi methodology. *Sādhanā*, *48*(1), 1.

[2] Bleicher, F., Reiter, M., & Brier, J. (2019). Increase of chip removal rate in single-lip deep hole drilling at small diameters by low-frequency vibration support. *CIRP Annals*, *68*(1), 93-96.

[3] Pelayo, G. U., Olvera-Trejo, D., Luo, M., Tang, K., De Lacalle, L. L., & Elías-Zuñiga, A. (2021). A model-based sustainable productivity concept for the best decision-making in rough milling operations. *Measurement*, *186*, 110120.

[4] Alaba, E. S., Kazeem, R. A., Adebayo, A. S., Petinrin, M. O., Ikumapayi, O. M., Jen, T. C., & Akinlabi, E. T. (2023). Evaluation of palm kernel oil as cutting lubricant in turning AISI 1039 steel using Taguchi-grey relational analysis optimization technique. *Advances in Industrial and Manufacturing Engineering*, *6*, 100115.

[5] Okokpujie, I. P., & Tartibu, L. K. (2021). Performance investigation of the effects of Nano-Additive-Lubricants with cutting parameters on material removal rate of AL8112 Alloy for advanced manufacturing application. *Sustainability*, *13*(15), 8406.

[6] Usluer, E., Emiroğlu, U., Yapan, Y. F., Kshitij, G., Khanna, N., Sarıkaya, M., & Uysal, A. (2023). Investigation on the effect of hybrid nanofluid in MQL condition in orthogonal turning and a sustainability assessment. *Sustainable Materials and Technologies*, *36*, e00618.

[7] Han, C., Luo, M., Zhang, D., & Wu, B. (2018). Iterative learning method for drilling depth optimization in peck deep-hole drilling. *Journal of Manufacturing Science and Engineering*, *140*(12), 121009.

[8] Araujo, A. C., Fromentin, G., & Blandenet, P. (2020). Investigation on PCD cutting edge geometry for Ti6Al4V high-feed milling. *The International Journal of Advanced Manufacturing Technology*, *111*, 1785-1796.

[9] Pelayo, G. U., & Trejo, D. O. (2020). Model-based phase shift optimization of serrated end mills: Minimizing forces and surface location error. *Mechanical Systems and Signal Processing*, *144*, 106860.

[10] Yang, H., Chen, Y., Xu, J., Ladonne, M., Lonfier, J., & Ding, W. (2020). Chip control analysis in low-frequency vibration-assisted drilling of Ti–6Al–4V titanium alloys. *International Journal of Precision Engineering and Manufacturing*, *21*, 565-584.

[11] Yılmaz, B., Karabulut, Ş., & Güllü, A. (2020). A review of the chip breaking methods for continuous chips in turning. *Journal of Manufacturing Processes*, *49*, 50-69.

[12] Benjamin D. M., Sabarish V. N., Hariharan M. V., Raj D. S. (2018) On the benefits of sub-zero air supplemented minimum quantity lubrication systems: an experimental and mechanistic investigation on end milling of Ti-6-Al-4-V alloy. Tribol Int 119:464–473.

[13] Kalyon, A., Günay, M., & Özyürek, D. (2018). Application of grey relational analysis based on Taguchi method for optimizing machining parameters in hard turning of high chrome cast iron. *Advances in Manufacturing*, *6*(4), 419-429.

[14] Liu, Y., Guo, L., Gao, H., You, Z., Ye, Y., & Zhang, B. (2022). Machine vision based condition monitoring and fault diagnosis of machine tools using information from machined surface texture: A review. *Mechanical Systems and Signal Processing*, *164*, 108068.

[15] Chen, S. H., Ge, Q., Zhang, J. S., Chang, W. J., Zhang, J. C., Tang, H. H., & Yang, H. D. (2021). Low-speed machining of a Zr-based bulk metallic glass. *Journal of Manufacturing Processes*, *72*, 565-581.

[16] Koech, G. K. (2019). *Investigation and application of artificial intelligence algorithms for complexity metrics based classification of semantic web ontologies* (Doctoral dissertation, Vaal University of Technology).